

# Stochastic modelling of reservoir sedimentation in a semi-arid watershed

*N. Adam, S. Erpicum, P. Archambeau, M. Pirotton, B. Dewals*

<sup>1</sup> *Hydraulics in Environmental and Civil Engineering (HECE), University of Liege (ULg)*

## Abstract

Sedimentation in large reservoirs is a major concern in semi-arid regions characterized by severe seasonal water scarcity. As a contribution to improved sediment management, this study analyses the real case of the reservoir of Sidi Yacoub in the north of Algeria. First, a dynamic model of the reservoir was set up and used to estimate past water and sediment inflows (period 1990-2010) based on data recorded by the dam operator and measurements at a gauging station located downstream of the reservoir. Second, in a stochastic framework using the statistical characteristics of inflow and outflow discharges, a projection of future sedimentation was performed until 2030, assuming stationarity of the statistical distributions. Third, the model was used to investigate the influence of possible climate change and to quantify the positive effects of soil conservation measures upstream.

## 1 Introduction

Reservoir sedimentation is a challenging issue worldwide (Morris and Fan 1998). The volume of sediment deposits is now growing faster than the overall storage capacity, leading to a yearly decrease in net storage by 1-2% (ICOLD-CIGB 2009). The consequences are numerous, including in terms of safety and ecological impacts (Lenhardt et al. 2009). Mitigating reservoir sedimentation and improving sediment management in reservoirs will remain a priority for the decades to come (Annandale 2011). In different parts of the world, sediment removal by hydraulic operations (flushing, sluicing ...) proved to be efficient (Tate and Farquharson 2000, Khan et al. 2012). Together with mitigation actions, such as soil conservation in the watershed and derivation or throughflow of turbid inflows during floods (Wan et al. 2010), sediment removal techniques may generally be successfully implemented to enable sustainable reservoir operation.

In contrast, achieving sustainable sediment management in semi-arid regions, such as the Mediterranean area, is far more complex. Long drought periods followed by heavy precipitations lead to particularly high erosion rates in the watersheds (Achite and Meddi 2004, Al-Ansari et al. 2013, Alaoui Mhamdi 2007, Molina-Navarro et al. 2014). In addition, the derivation of flood flows and the removal of sediment deposits by hydraulic techniques may hardly be implemented due to severe water scarcity in these regions. This contributes to the accumulation of large sediment volumes in the reservoirs. For instance, in 2000, the mean volume of sediment deposits in Algerian reservoirs exceeded 20 % of their initial capacity. This share is similar in most of the Maghreb (Mammou and Louati 2007) and leads to highly critical conditions for the socio-economic development of these countries (Benblidia et al. 2001, Boudjadja et al. 2003).

In this study, we analysed the sedimentation taking place in the Sidi Yacoub reservoir, located on the oued Ardjem (Algeria), which is a tributary of the oued Chlef flowing into the Mediterranean Sea. The dam was commissioned in 1986 and, in 2004, the amount of sediment deposits reached 10 % of the initial storage capacity (Hydrodragage and C.T.Systems 2004). The goal of the study is to analyse future sedimentation in the Sidi Yacoub reservoir using a stochastic approach. A dynamic model of the reservoir has been set up based on daily management data of the dam and measurements at a gauging station. The model was calibrated and validated using field data.

The study is divided into three steps. First, the model was run for the period 1990-2010 (*reference period*) to estimate past water and sediment inflows. From recorded flood data, a power relation between water and sediment inflows was derived and validated against measurements (Belhadri 1997). Second, the model was run for the period 2010-2030 (*projection period*) to investigate future sedimentation in the reservoir. Based on the statistical characteristics of past inflows, the statistical distribution of the volume of sediment deposits was computed for the period 2010-2030. Third, the model was used to appreciate the influence on reservoir sedimentation of possible climate evolutions or mitigation measures such as soil conservation in the watershed.

The main novelty of the paper is the statistical approach developed to characterize the water inflows and outflows. This approach is new, it enables a high level of detail in the reproduction of the variability of the time series and, yet, it remains very flexible so that it may easily be transferred to other case studies. As a result, long term projections of future sedimentation could be performed in a truly stochastic framework, whereas many recent studies either focused on the past, especially when detailed 2D models were involved (Molino et al. 2001, Kouassi et al. 2013), or rerun past time series to investigate future sedimentation (Tate and Farquharson 2000).

Section 2 presents the study area and available data. The developed model is detailed in section 3, together with the estimation of water and sediment inflows during the period 1990-2010. The statistical characterization of in- and outflows is presented in section 4, as an onset for modelling future reservoir sedimentation. Finally, the results are presented and discussed in section 5.

## 2 Case study description

### 2.1 Study area

The Sidi Yacoub watershed covers 920 km<sup>2</sup>. It belongs to the Chlef watershed in North Algeria (between Oran and Alger). It is located in a Mediterranean semi-arid region, between 35° and 36° north latitude, and 1°15' and 1°45' east meridian (TECSULT 2006). The elevations in the watershed lie between 1200 m (in the Ouarsenis mountains) and about 190 m in the reservoir. This area is composed of 10 % without vegetation, 20 % of forest area, 30 % of farmed land and the other 40 % is scrubland. Forest areas are mostly on erosion-resistant soil, while farmed areas are mainly on relatively steep slopes (TECSULT 2006). The geology of the watershed is composed of recent sediments from the Quaternary period (in the south-east part of the watershed), limestone and marlstone from Trias and Neogene (mountainous areas).

The regional Mediterranean climate is characterised by distinctive wet and dry seasons. The mean daily inflow over the studied period (1990-1991 to 2009-2010) is 1.5 m<sup>3</sup>/s, while the mean daily inflows during the wet and dry seasons are respectively 2 m<sup>3</sup>/s and 0.3 m<sup>3</sup>/s. The maximum daily discharge is 222 m<sup>3</sup>/s. Like in many parts of the world, the north of Algeria undergoes inter-annual climatic variations (Frossard et al. 2006, Martin et al. 2009, Meddi and Meddi 2009). A relatively dry period has started in this area since the 1970s, with a mean annual discharge about 30 % below the long term mean value.

The construction of the Sidi Yacoub embankment dam started in 1981 and was completed in 1986. The initial capacity of the reservoir was 286 hm<sup>3</sup>. Most reservoir management data are available only from September 1990. A bathymetric survey performed in 2004 revealed that the storage capacity at this time had decreased by 33 hm<sup>3</sup>. The mean annual aggradation rate is about 1.9 hm<sup>3</sup>/yr. (Hydrodragage and C.T.Systems 2004). The deposits consist mostly of fine silt (mean grain size of 10 µm to 30 µm), with a very limited fraction of sand (Belhadri 1997). According to the regional water authorities, mitigation of soil erosion in the upstream watershed is thought to be the most efficient approach to enhance sediment management (TECSULT 2007).

## 2.2 Available data

Three types of data were used in this study. They consist in: (i) measurements at a gauging station downstream of the dam; (ii) data collected on-site by the dam operator and (iii) topographic maps as well as a bathymetric survey.

For the period 1985 to 2010, the water and sediment discharges were recorded at a hydrometric station (“01 23 11”, oued Ben Aek CD 73) located on oued Sly (downstream of the dam). As there is a tributary between the dam and this station, these records could not be used directly in the mass balance of the reservoir; but we used them to derive a transport capacity formula. The time step ranges between 10 minutes (during floods) and one day (during non-flood periods). The flow discharge and sediment transport rate were not always measured simultaneously. Complete flow data at this station cover only 5 % to 10 % of the total time (Elalmi 2013).

Daily pool levels and outflow discharges were recorded by the dam operator. The data series is complete from 1<sup>st</sup> September 1990 to 31<sup>st</sup> August 2010. Four contributions may be distinguished in the outflow discharge:

- Irrigation and water supply represent nearly 75 % of the total outflow. As shown in Figure 1(a), this component of the outflow is highly dependent on the season. Indeed, the 20-year average of daily values during the dry season exceeds 2 m<sup>3</sup>/s, whereas the average daily discharge during the wet season remains almost constant, at a value of approximately 0.2 m<sup>3</sup>/s.
- The evaporation corresponds to more than 23 % of the total outflow. The 20-year average of daily evaporation depths follows a regular pattern, ranging between 0.002 m during the wet season and 0.01 m during the dry season (Figure 1-b). The evaporation depth is evaluated here as the ratio between the daily mean evaporation outflow, as estimated by the dam operator, and the daily mean of the reservoir area.
- Representing about 1 % of the total outflow, the leakage was assumed constant by the dam operator, at an average daily value of 0.01 m<sup>3</sup>/s.

- The bottom outlet discharge represents also about 1 % of the total outflow. No distinctive operation rules could be inferred from the records of operation of the bottom outlet.

Pre-impoundment bathymetric data were obtained by digitalization of old topographic maps, while the bathymetry in 2004 was provided by a bathymetric survey of the reservoirs (Hydrodragage and C.T.Systems 2004). These two bathymetric models are illustrated in Online Resource 1, while the corresponding stage-storage and stage-surface relationships are given in Figure 2.

### 3 Estimation of water and sediment inflows in the past

Reliable estimates of sediment inflow constitute key input data to predict and manage reservoir sedimentation; but they are also particularly difficult to obtain. Here, we developed a dynamic model of the reservoir to estimate the inflows from the time evolution of the pool level and the known water outflows. These are the only time series available from the monitoring performed by the dam operator. They cover the period 1990-2010 (referred to hereafter as the *reference period*).

#### 3.1 Dynamic model of the reservoir

A dynamic model of the reservoir has been set up. It solves the mass balance of water and sediments in the reservoir using the continuity equation for the water-sediment mixture integrated over the whole reservoir:

$$\frac{dV_{tot}}{dt} = Q_{IN}^w - Q_{OUT}^w + Q_{IN}^s - Q_{OUT}^s, \quad (1)$$

where  $V_{tot}$  [m<sup>3</sup>/s] represents the total volume in the reservoir (water and sediments),  $Q_{IN/OUT}^w$  [m<sup>3</sup>/s] the liquid in- and outflow, and  $Q_{IN/OUT}^s$  [m<sup>3</sup>/s] the sediment in- and outflow.

Equation (1) was discretized as follows, using time steps  $\Delta t$  of one day:

$$V_{tot}(t + \Delta t) - V_{tot}(t) = \left[ Q_{IN}^w(t + \frac{\Delta t}{2}) - Q_{OUT}^w(t + \frac{\Delta t}{2}) + Q_{IN}^s(t + \frac{\Delta t}{2}) - Q_{OUT}^s(t + \frac{\Delta t}{2}) \right] \Delta t, \quad (2)$$

where  $Q_{IN/OUT}^{w/s}(t + \frac{\Delta t}{2})$  refers to an average value between time  $t$  and time  $t + \Delta t$ .

#### 3.2 Sediment in- and outflows

In equation (2), three fluxes are unknown:  $Q_{IN}^w$ ,  $Q_{IN}^s$  and  $Q_{OUT}^s$ . Therefore, two additional closure relations are needed. First, a power relation was used to link the sediment mass discharge  $Q^s$  [kg/s] and the flow volumetric discharge  $Q^w$  [m<sup>3</sup>/s]:

$$Q^s = \alpha (Q^w)^\beta \quad (3)$$

The parameters  $\alpha$  and  $\beta$  were fitted by the least square method, based on the flow and sediment discharges measured at the gauging station “01 23 11” (downstream of Sidi Yacoub dam) during eight large floods (Online Resource 2). This led to the value of  $\beta = 1.31$  for the exponent, which is very consistent with values given by Achite and Meddi (2004) for similar watersheds in Algeria. Initially estimated at 15.7, the coefficient  $\alpha$  was recalibrated to 35.8, so that a run of the reservoir model between 1990 and 2004 leads to a computed volume of sediment deposits consistent with the bathymetric survey performed in 2004 (Hydrodragage and C.T.Systems 2004).

Second, the trapping efficiency ( $TE$ ) formula of Churchill was used to deduce the sediment outflow (Espinosa-Villegas and Schnoor 2009):

$$TE = \frac{Q_{OUT}^s}{Q_{IN}^s} = 1 - \frac{800SI^{-0.2} - 12}{100}, \quad \text{with} \quad SI = \frac{(C/I)^2}{L}, \quad (4)$$

where  $C$  is the reservoir capacity [ $m^3$ ],  $I$  the inflow [ $m^3/s$ ] and  $L$  a characteristic length [ $m$ ]. The characteristic length  $L$  was estimated as the square root of the reservoir surface area.

The computations performed for the period 1990-2010 showed that the trapping efficiency does not take values below 99 %. Hence, the sediment outflow  $Q_{OUT}^s$  was neglected in the resolution of equation (2), which reduces thus to:

$$V_{tot}(t + \Delta t) - V_{tot}(t) = \left[ Q_{IN}^w(t + \frac{\Delta t}{2}) - Q_{OUT}^w(t + \frac{\Delta t}{2}) + \alpha \left( Q_{IN}^w(t + \frac{\Delta t}{2}) \right)^\beta \right] \Delta t. \quad (5)$$

Since  $V_{tot}$  and  $Q_{OUT}^w$  are known at every time step from 1990 to 2010, from data recorded by the dam operator, the only remaining unknown is  $Q_{IN}^w$ . At each time step, the non-linear relation (5) was solved for  $Q_{IN}^w$  using a standard Newton-Raphson technique.

To summarize, the complete resolution procedure involves three steps:

1. the continuity equation (5) was solved to find the liquid inflow  $Q_{IN}^w$  ;
2. using relation (3) and the trapping efficiency formula (4), the volume  $V_{sed}$  of sediment deposits in the reservoir was deduced;
3. finally, the remaining water storage capacity in the reservoir was computed from  $V_w(t) = V_{tot}(t) - V_{sed}(t)/(1 - p)$  where  $p$  is the porosity of the deposits, assumed equal to 0.35.

### 3.3 Results

The model was first run for the period 1990-1994 and the predicted volumes of sediment deposits were compared with estimated volumes from Belhadri (1997) for the years 1990-1991 to 1993-1994. As shown in Figure 3, the computed and estimated volumes show a similar sequence of years with higher vs. lower sediment inflows. In addition, the maximum difference between computed and estimated values ( $\sim 0.25 \text{ hm}^3$ ) remains below 15 % of the mean annual sediment inflow.

Next, the model was run for the whole reference period (1990-2010). The evolution of the computed water inflows is shown in Figure 4(a), highlighting a high variability, with a few floods and many small daily inflows. While the average inflow is about 1.5 m<sup>3</sup>/s, the maximum inflow exceeds 220 m<sup>3</sup>/s. Some non-physical negative daily “inflows” are obtained, most probably as a result of errors or simplifying assumptions in the data recorded by the dam operator.

Figure 4(b) represents the time series of computed inflows per hydrological year, revealing the existence of a dry season during the last 110 days of each year. This distinctive feature of the flow regime was used in the development of the methodology for computing sedimentation during the projection period, as detailed in section 4. The seasonal pattern observed in Figure 4(b) also confirms the relevance of defining the hydrological year from 1<sup>st</sup> September to 31<sup>st</sup> August.

Based on these results, neither a significant trend in climate evolution nor climate oscillations could be identified over the reference period. This is partly due to the relatively short length of the time series, covering only 20 years.

## 4 Future reservoir sedimentation

The projection of future sedimentation in the reservoir was performed in two steps:

1. the time series of past inflows and outflows were characterized statistically;
2. a high number of runs of the dynamic model of the reservoir were performed by feeding the model with input data (inflow and outflow volumes) respecting the statistical characteristics of the past time series.

As a result, a statistical distribution was obtained for the volume of sediment deposits in the Sidi Yacoub reservoir at each daily time step in the future.

### 4.1 Statistical characterization of reservoir inflow and outflow

From the previous step of the analysis (section 3), the time series of estimated daily inflow volumes into the reservoir are known for the period 1990-2010, while the time series of outflow are directly available from data collected by the dam operator (section 2.2). To predict future sedimentation in the reservoir, similar time series of inflow and outflow volumes are needed for the period 2010-2030 and beyond (referred to as the *projection period*). Here, we assumed that the statistical characteristics of these future time series remain the same as those of the past, consistently with a stationarity assumption (Tate and Farquharson 2000).

#### *Outflow volumes*

As detailed in section 2.2, the reservoir outflow can be split into four contributions: irrigation and water supply, evaporation, bottom outlet releases and leakage.

The outflow for irrigation and water supply varies with the season, as shown in Figure 1(a). This behaviour was reproduced by estimating the corresponding outflow volume  $Q_{OUT}^{ws}$  during any day  $d$  of a year  $N$  in the future as follows:

$$Q_{OUT}^{ws} = [Q_{OUT}^{ws}]_{50}^d + \frac{|\zeta_N| + \zeta_N}{2} \left( [Q_{OUT}^{ws}]_{75}^d - [Q_{OUT}^{ws}]_{50}^d \right) - \frac{|\zeta_N| - \zeta_N}{2} \left( [Q_{OUT}^{ws}]_{50}^d - [Q_{OUT}^{ws}]_{25}^d \right), \quad (6)$$

where  $[Q_{OUT}^{ws}]_j^d$  refers to the  $j^{\text{th}}$  percentile of the outflow volume of day  $d$  during the reference period (1990-2010).  $\zeta_N$  is a random number following a standard normal distribution. Eq. (6) expresses that the average annual pattern of the outflow volumes for irrigation and water supply is scaled for each year in the future. This enables to preserve the existing correlations between daily outflow volumes within a year, as revealed by the available data for the reference period.

For any day  $d$  in a year  $N$  of the projection period, the daily evaporation volume is calculated as the product between the current surface area of the reservoir (Figure 2-b) and an evaporation depth deduced from data available for the reference period 1990-2010 (Figure 1-b). Indeed, the 20-year averages of the daily evaporation depths during the reference period follow a distinct and relatively regular pattern as a function of the day of the year, as shown by the black curve in Figure 1(b). Therefore, a simple polynomial relationship (red curve in Figure 1-b) was fitted to provide the daily evaporation depth as a function of the index of the day in the year.

The bottom outlet releases and the leakage volume represent a share of less than 6 % in the total outflow for the reference period. In addition, no clear correlation could be found with other state variables of the reservoir. Therefore, these two contributions were assumed to remain constant for the projection period. The estimated values for the bottom outlet outflow and the “leakage” outflow are, respectively, 0.01 m<sup>3</sup>/s and 0.05 m<sup>3</sup>/s. The latter value accounts also for the computed “negative inflows”, as mentioned in section 3.3.

### *Inflow volumes*

The inflow volumes show a very high variability, involving many zero or quasi zero daily inflows as well as a number of major flood events (Figure 4). Therefore, the construction of the series of future inflows handles separately the flood days from the other days. Hence, it consists in two main parts:

- part 1: compute the inflow for “dry days” (i.e. days with zero inflow) and for “normal” days (i.e. neither a flood day, nor a “dry” day);
- part 2: determine the inflows during flood days.

In turn, part 1 is divided into several sub-parts, as detailed in the flow chart in Figure 5:

- estimate the annual mean inflow of the current year (sub-part 1.1),
- estimate the seasonal mean inflow during the current wet season (sub-part 1.2),
- determine the number of flood days during the current year (sub-part 1.3), as necessary to conduct sub-part 1.5 and part 2,
- for the wet season, determine whether the current day is “dry” or not and estimate the inflow for “normal” days (sub-part 1.4)
- estimate the seasonal mean inflow during the dry season (sub-part 1.5),
- for the dry season, similarly to sub-part 1.3, determine whether the current day is “dry” or not and estimate the inflow for “normal” days (sub-part 1.6).

More details on the statistical distributions used in each part are given as electronic supplementary material in Online Resource 3.

**Sub-part 1.1** The annual mean  $\langle Q \rangle_Y$  for any year  $Y$  of the projection period was computed as:  $\langle Q \rangle_Y = \gamma_Y$ , with  $\gamma_Y$  a random variable following a Weibull distribution. The parameters of this distribution were deduced from the inflow time series during the reference period (Online Resource 3).

**Sub-part 1.3** For each year, the seasonal mean inflow during the wet season was estimated from a statistical distribution fitted on the difference  $\Delta Q_S$  between the seasonal mean inflow  $\langle Q \rangle_W$  and the annual mean inflow of the corresponding year, scaled by the mean annual inflow:  $\Delta Q_S^W / \langle Q \rangle_Y$ . Hence, the seasonal mean inflow during the wet season is given by:  $\langle Q \rangle_W = \langle Q \rangle_Y (1 + \gamma_S^W)$ , where  $\gamma_S^W$  is a random variable following a generalized extreme value distribution fitted based on the time series of inflows computed for the reference period (Online Resource 3).

**Sub-parts 1.4 and 1.6** At the beginning of each daily time step, during both the wet and the dry seasons, a third random variable is used to determine whether the current daily inflow is zero or not. This random variable follows a uniform distribution between 0 and 1. If its value is below a given threshold, then the inflow is simply set to 0. Otherwise, the procedure to determine the daily inflows is continued. The threshold values depend on the season. Based on the results detailed in section 3.3, they were set to 12 % for the wet season and 42 % for the dry season.

Next, for any “normal” day  $d$  during a season  $S$  (wet or dry) of a year  $Y$ , the “normal” daily inflow  $Q_d$  is expressed as the sum of three components:

1. the annual mean inflow of the current year  $Y$ :  $\langle Q \rangle_Y$ ,
2. the difference between the seasonal mean inflow  $\langle Q \rangle_S$  of the current season  $S$  and the annual mean inflow  $\langle Q \rangle_Y$ :  $\Delta Q_S = \langle Q \rangle_S - \langle Q \rangle_Y$ ,
3. and, the difference between the daily inflow of the current day  $d$  and the seasonal mean inflow  $\langle Q \rangle_S$ :  $\Delta Q_d = Q_d - \langle Q \rangle_S$ .

This decomposition into three components leads to the following expression for  $Q_d$ :

$$Q_d = \langle Q \rangle_Y + \Delta Q_S + \Delta Q_d. \quad (7)$$

Consequently, to perform the projection of future sedimentation in the reservoir, the following four random variables  $\gamma_Y$ ,  $\gamma_s^w$ ,  $\gamma_d^w$  and  $\gamma_d^D$  were used:

$$\gamma_Y = \langle Q \rangle_Y ; \gamma_s^w = \frac{\Delta Q_S^w}{\langle Q \rangle_Y} ; \gamma_d^w = \frac{\Delta Q_d^w}{\langle Q \rangle_S^w} \text{ and } \gamma_d^D = \frac{\Delta Q_d^D}{\langle Q \rangle_S^D}. \quad (8)$$



Using this decomposition was motivated by the significantly better fit of statistical distributions for the random variables defined in Eq. (8) than directly for the variable  $Q_d$ . The obtained distributions and their performance are documented in Online Resource 3.

Hence, the daily inflow  $Q_d$  during any “normal” day, during the wet season, was expressed as:

$$Q_d = \gamma_Y (1 + \gamma_S^W)(1 + \gamma_d^W). \quad (9)$$

**Sub-part 1.5** For each year in the projection period, the average dry season inflow  $\langle Q \rangle_s^D$  was deduced from the current annual mean and the wet season mean inflows, to preserve the annual mean inflow:

$$\Delta Q_s^D = -\frac{T_{WS}}{T_{DS}} \gamma_S^W \gamma_Y \quad (10)$$

**Sub-part 1.6** As a result, the daily inflow during any “normal” day of future dry seasons is given by:

$$Q_d = \gamma_Y \left( 1 - \frac{T_{WS}}{T_{DS}} \gamma_S^W \right) (1 + \gamma_d^D) \quad (11)$$

with  $\Delta Q_s^D$  the average dry season inflow variation and  $T_s^{D/W}$  the duration of the dry/wet season, excluding zero-inflow and flood days. The mean duration of the wet season is 255 days (including zero and flood days), as deduced from the results displayed in Figure 4(b) (see section 3.3).

**Part 2** The flood inflows during a year  $N$  of the projection period are evaluated in two steps: first, the annual maximum inflow of year  $N$  is determined; second the other flood inflows of the year are deduced.

- To estimate the maximum flood inflow for each year  $N$  of the projection period, a random variable following a standard uniform distribution was used to distinguish between two cases. If this variable takes a value below 0.5 for the year  $N$ , the maximum discharge of this year is assumed to correspond to a return period higher than 2 years, and vice-versa if the value of the random variable is above 0.5. In the former case, the maximum annual inflow is deduced from a Gumbel distribution, which was fitted on the annual maximum inflows for the reference period (root mean square error of 8 %). In the latter case, the annual maximum inflow was deduced from the distribution of flood discharges characterizing the reference period (Online Resource 3).
- Based on the number of flood days during the current year, as estimated in sub-part 1.3, the corresponding flood discharges (below the annual maximum discharge) are determined using a random variable and the distribution of flood discharges for the reference period, truncated below the maximum annual inflow of the current year (Online Resource 3).

## 4.2 Results and discussion

Once the different in- and outflows were determined, formulation (2) of the reservoir model was solved again to estimate the time-evolution of the volume of sediment deposits during the projection period. At this stage, all inflow and outflow discharges were known from the random statistical

distributions as well as relations (9) and (11). The sediment discharges were deduced from equations (3) and (4) (section 3).

As detailed in Online Resource 3, the computed future water inflows were verified considering a 100,000 year projection period, assuming that all statistical parameters are kept constant. A good agreement was obtained between the statistical distributions of projected values and data of the reference period. This confirms the ability of the model to reproduce the variability of the hydrological regime in the Sidi Yacoub reservoir. The statistical characteristics of all data distributions are well reproduced by the projection algorithm; except for the dry season. This results from relation (10), which uses the dry season inflows to ensure a correct mean annual inflow and does not explicitly reproduce the statistical distribution of the seasonal mean during the dry season. However, the sediment inflows during the dry season are obviously much smaller than during the rest of the year and, therefore, the dry season plays a minor part in the overall results.

Following a Monte-Carlo approach, the projection of future volumes of sediment deposits was based on 1,000 runs of the reservoir model. Figure 6 shows the time evolution of the volume of sediment deposits for the reference period (1990-2010) and for the projection period (2010-2030). Three specific runs, selected randomly, are also displayed. They confirm the ability of the model to reproduce the high variability of the inflows, inducing sudden rises in the volume of sediment deposits.

The results show that the volume of sediment deposits in 2030 is expected to be between 70 hm<sup>3</sup> and 105 hm<sup>3</sup>, with a mean value of 87 hm<sup>3</sup>. This represents 24 % to 37 % of the initial reservoir capacity.

Since the mean annual inflow was assumed to remain constant (scenario A), the average result of the present model is very close to the result of a simple linear extrapolation of past rates of sediment deposits (Figure 6-a). Nonetheless, the present dynamic model enables the uncertainty range of future sedimentation rates to be assessed, which would not have been possible from a simple mathematical extrapolation.

## 5 Discussion

The model developed here takes explicitly into account the sediment inflow in the resolution of the continuity equation. In contrast, neglecting the sediment inflow during the 1990-2010 period, which makes the problem linear, leads to an overestimation of the water inflow by about 10 %. Moreover, neglecting the sediment inflow in the resolution of the model increases the occurrence of non-physical negative values in the computed inflows by about 15 %.

Generally, the rate of sediment deposition is expected to gradually decrease with time, as the trapping efficiency progressively declines. This is reproduced in the present model by means of equation (4), but it turns out not to have any significant influence on the results for the considered projection period (2010-2030), as the computed rate of sedimentation is found to remain essentially the same as during the reference period (Figure 6-a). In contrast, if the projection period is extended beyond 2030, the effect of a decreasing trapping efficiency becomes visible in the results, as shown

in Figure 7. Here also, extrapolating based on the assumption of a constant sedimentation rate does not provide any insight into the variability range of future volumes of sediment deposits.

According to Meddi and Meddi (2009), interannual climatic variability in the north-west of Algeria is characterized by a sequence of wet and dry periods. A dry period started in 1980 and continued until 2003. Meddi and Meddi (2009) report a decrease in precipitation by 35 % between the wet and the dry climate periods (around 1980) for the oued Sly, which is the name of oued Ardjem downstream of its junction with the tributary oued Lag (downstream of the dam). The model was re-run to appreciate the effect of this type of variation in climate. Figure 8(a) (scenario B) shows the computed volumes of sediment deposits assuming a sudden increase by 50 % in annual water inflows from the year 2010 (Meddi and Hubert 2003). The mean value of sediment deposits is found to increase in approximately the same proportion.

To investigate the sensitivity of the modelling results, a different scenario of climate evolution was considered. It involves an intensification of wet hydrological extremes: the annual flood discharges were assumed to increase by 15 % (scenario C), without changes in the distribution of “normal” inflow (section 4). The computed upper bound of sedimentation volumes increases by 55 % (Figure 8-a), while the lower bound is not affected; and the mean value changes by no more than 10 hm<sup>3</sup> (11 %). This highlights the decisive role of floods in the overall sedimentation process.

The model set up here may also be used to guide sediment management. As recommended by TECSULT (2007), erosion control in the watershed is expected to be the most effective measure to reduce sedimentation in the reservoir. A risk assessment model may be used to identify the most critical erosion-prone areas in the watershed (Chen et al 2011) and soil conservation measures, such as the promotion of more appropriate vegetation types (Shuka et al. 2011, Pradhan et al. 2010), should be implemented. By means of a change in the coefficient  $\alpha$ , the present model can be used to assess the influence of a given reduction in sediment inflows. Scenario D in Figure 8(b) corresponds to a sudden decrease by 40 % in the sediment inflows, which is shown to have a major effect on the deposited volume in 2030. More realistically, a progressive decrease of erosion was tested. This scenario corresponds to a 10 % decrease after 5 years, 20 % after 10 years and 40 % after 15 years (scenario E in Figure 8-b). Figure 8(b) quantifies the significant benefit of reducing sediment yield for ensuring a more sustainable operation of the reservoir.

## 6 Conclusion

Algeria and the Maghreb are severely affected by sedimentation in their surface water reservoirs. A dynamic model was developed and applied to the case of the Sidi Yacoub reservoir. This model takes into account the sediment inflows by means of a power relation.

The model was first used to estimate the inflows during the past 20 years of operation of the reservoir. Next, the model was applied in a stochastic framework to analyse the future evolution of sediment deposits in the reservoir, assuming stationarity of the characteristics of 1990-2010 inflows and outflows. In contrast with simple mathematical extrapolations of past sedimentation rates, the present stochastic modelling also provides a quantification of the uncertainty range of future

sedimentation rates. This information is of particularly high relevance to guide decision-making for optimal and sustainable sediment management in the reservoir.

Finally, the model was used to quantify the effect of different scenarios of future variations in climate, as well as to assess the influence on sedimentation rates of different erosion-reduction measures on the watershed. Due to its flexibility and its physical basis, the model may be easily transferred to analyse other case studies.

## Acknowledgement

The authors acknowledge Bakhta Chenaoui from the University of Chlef (Algeria) for the data provided, as well as Marc Binard from the University of Liege (ULg) for his support in the digitalization of topographic maps corresponding to the pre-impoundment conditions.

## References

- Achite, M. and M. Meddi (2004). Estimation du transport solide dans le bassin-versant de l'oued Haddad (Nord-Ouest algérien). *Sécheresse*, 15: 367-373.
- Al-Ansari, N., I.E. Issa, G. Sherwani and S. Knutsson (2013). Sedimentation in the mosul reservoir of northern Iraq. *Journal of Environmental Hydrology*, 21(7): 1-10.
- Alaoui Mhamdi, B., Azzouzi, A., Alaoui Mhamdi, M. & Sime-Ngando, T. 2007. Dynamics of the relative nitrogen and phosphorus concentrations in a reservoir situated in a semi-arid zone (Sahela, Morocco). *Water Resources Management*, 21, 983-995.
- Annandale, G. (2011). Going full circle. *International Water Power and Dam Construction*, 63(4): 30-34.
- Belhadri, M. (1997). Caractérisation et valorisation de la vase du barrage de Sidi Yacoub. Master thesis, Univeristy of Chlef.
- Benblidia, M., A. Salem and A. Demmak (2001). Extraction des sédiments dans les retenues. *La houille blanche*, (6-7): 76-78.
- Boudjadja, A., M. Messahel and H. Pauc (2003). Ressources hydriques en Algérie du Nord. *Revue des sciences de l'eau/Journal of Water Science*, 16(3): 285-304.
- Chen, L., X. Qian and Y. Shi (2011). Critical area identification of potential soil loss in a typical watershed of the Three Gorges reservoir region *Water Resources Management*, 25:3445-3463.
- Elalmi, T. (2013). Evaluation de la ressource en eau superficielle (bilan hydriques des bassins versants du nord de l'algerie). Master thesis, University of Kasdi Merbah Ouargla.
- Espinosa-Villegas, C. O. and J. L. Schnoor (2009). Comparison of long-term observed sediment trap efficiency with empirical equations for Coralville Reservoir, Iowa. *Journal of Environmental Engineering*, 135(7): 518-525.

- Frossard, E., H. Garros-Berthet and S. Le Clerc (2006). Évolution des régimes hydrologiques avec le climat: Incidences sur les aménagements hydrauliques. Transactions of the International Congress on Large Dam, 22(4): 521-542.
- Hydrodragage and C.T.Systems (2004). Leves bathymétriques des barrages en exploitation (Lots II et II: Echelon Cheliff et centre) - Barrage de Sidi Yacoub (Wilaya du Chlef), Agence nationale des barrages - Direction de la maintenance et du controle.
- ICOLD-CIGB (2009). Sedimentation and Sustainable Use of Reservoirs and River Systems, Pre-print ICOLD Bulletin n°147, ICOLD, Paris.
- Khan, N. M., Babel, M. S., Tingsanchali, T., Clemente, R. S. & Luong, H. T. 2012. Reservoir Optimization-Simulation with a Sediment Evacuation Model to Minimize Irrigation Deficits. Water Resources Management, 26, 3173-3193.
- Kouassi, K. L., Kouame, K. I., Konan, K. S., Sanchez Angulo, M., Deme, M. & Meledje, N. H. E. 2013. Two-Dimensional Numerical Simulation of the Hydro-Sedimentary Phenomena in Lake Taabo, Côte d'Ivoire. Water Resources Management, 27, 4379-4394.
- Lenhardt, M., Markovic, G. & Gacic, Z. 2009. Decline in the index of biotic integrity of the fish assemblage as a response to reservoir aging. Water Resources Management, 23, 1713-1723.
- Mammou, A. B. and M. H. Louati (2007). Évolution temporelle de l'envasement des retenues de barrages en Tunisie. Revue des sciences de l'eau/ Journal of Water Science, 20: 201-210.
- Martin, C., M. Meddi and A. Talia (2009). Évolution récente des conditions climatiques et des écoulements sur le bassin versant de la Macta (Nord-Ouest de l'Algérie). Physio-Géo. Géographie, physique, et environnement, 3: 61-84.
- Meddi, H. and M. Meddi (2009). Variabilité des précipitations annuelles du Nord-Ouest de l'Algérie. Science et changements planétaires/Sécheresse, 20(1): 57-65.
- Meddi, M. and P. Hubert (2003). Impact de la modification du régime pluviométrique sur les ressources en eau du nord-ouest de l'Algérie. IAHS Publication: 229-235.
- Molina-Navarro, E., Martínez-Pérez, S., Sastre-Merlín, A. & Bienes-Allas, R. 2014. Catchment Erosion and Sediment Delivery in a Limno-Reservoir Basin Using a Simple Methodology. Water Resources Management.
- Molino, B., Greco, M. & Rowan, J. S. 2001. A 2-D reservoir routing model: Sedimentation history of Abbeystead reservoir, U.K. Water Resources Management, 15, 109-122.
- Morris, G. L. and J. Fan (1998). Reservoir sedimentation handbook: design and management of dams, reservoirs, and watersheds for sustainable use, McGraw-Hill, New York.
- Pradhan, D., Ancev, T., Drynan, R. & Harris, M. 2010. Management of Water Reservoirs (Embungs) in West Timor, Indonesia. Water Resources Management, 25, 339-356.
- Shuka, L., Çullaj, A., Shumka, S., Miho, A., Duka, S. & Bachofen, R. 2011. The Spatial and Temporal Variability of Limnological Properties of Bovilla Reservoir (Albania). Water Resources Management, 25, 3027-3039.

- Tate, E. L. & Farquharson, F. a. K. 2000. Simulating reservoir management under the threat of sedimentation: The case of Tarbela dam on the River Indus. *Water Resources Management*, 14, 191-208.
- TECSULT (2006). Etude de la protection du bassin versant du barrage Sidi-Yacoub: Phase II - Description du milieu, Ministère des ressources en eau (Agence nationale des barrages - Direction de la maintenance et du contrôle).
- TECSULT (2007). Etude de protection du bassin versant du Barrage Sidi-Yacoub: Phase V - Avant projet détaillé et dossier d'appel d'offres, Ministère des ressources en eau (Agence nationale des barrages - Direction de la maintenance et du contrôle).
- Wan, X. Y., Wang, G. Q., Yi, P. & Bao, W. M. 2010. Similarity-Based Optimal Operation of Water and Sediment in a Sediment-Laden Reservoir. *Water Resources Management*, 24, 4381-4402.

## Notations

$C$	Reservoir capacity
$d$	Index referring to any given day
$I$	Reservoir inflow
$L$	Reservoir characteristic length
$P$	Sediment porosity
$Q_{IN}^s$	Sediment inflow
$Q_{OUT}^s$	Sediment outflow
$Q_{IN}^w$	Water inflow
$Q_{OUT}^w$	Water outflow
$Q_d$	Daily inflow
$Q_d^{W/D}$	Daily inflow during the wet / dry season
$\langle Q \rangle_Y$	Annual mean inflow for any year $Y$ of the projection period
$\langle Q \rangle_S^{W/D}$	Seasonal mean inflow during the wet / dry season
$S$	Reservoir area
$SI$	Sediment inflex from Churchill
$T_{WS}$	Duration of the wet season
$T_{DS}$	Duration of the dry season
$V_{sed}$	Sediments volume
$V_{tot}$	Total volume (water + sediments)
$V_w$	Water volume
$Y$	Index referring to a given year
$\alpha$	Factor in the relation between sediment discharge and water discharge
$\beta$	Exponent in the relation between sediment discharge and water discharge

$\zeta_N$	Random number following a standard normal distribution
$\gamma_Y$	Random variable representing the annual mean inflow
$\gamma_S^W$	Random variable representing the ratio $\Delta Q_S^W / \langle Q \rangle_Y$
$\gamma_d^{W/D}$	Random variable representing the ratio $\Delta Q_d^{W/D} / \langle Q \rangle_S^{W/D}$
$\Delta Q_S^{W/D}$	Difference between the seasonal mean inflow during the wet / dry season and the corresponding annual mean inflow
$\Delta Q_d^{W/D}$	Difference between the daily mean inflow during the wet / dry season and the corresponding seasonal mean inflow

# Figures

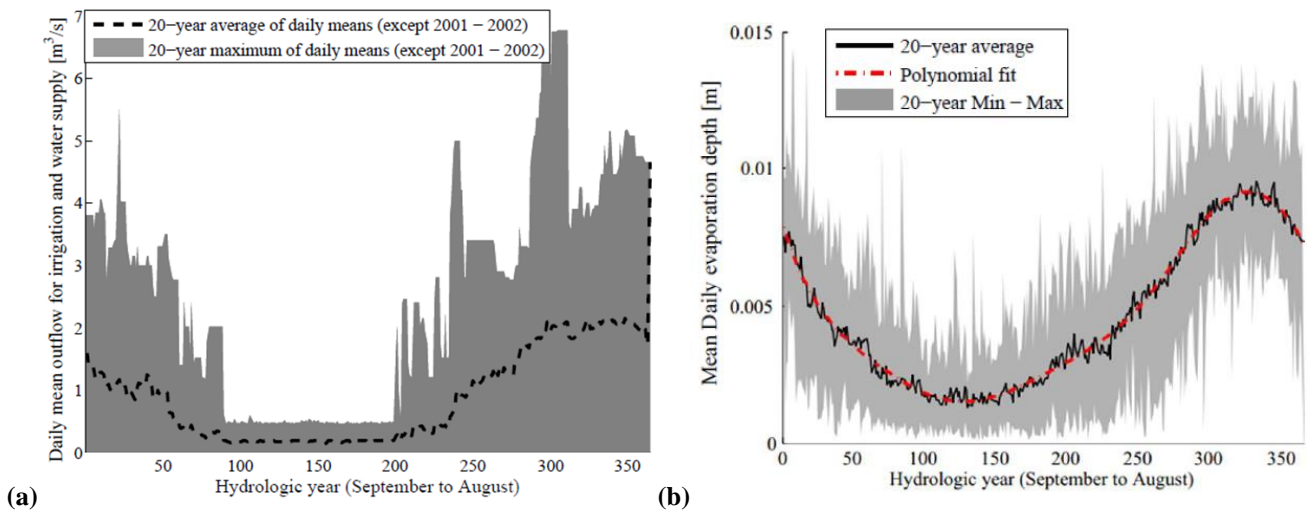


**Figure 1: Daily outflow for irrigation and water supply (a), and daily evaporation depths (b) during the reference period (1990-2010).**

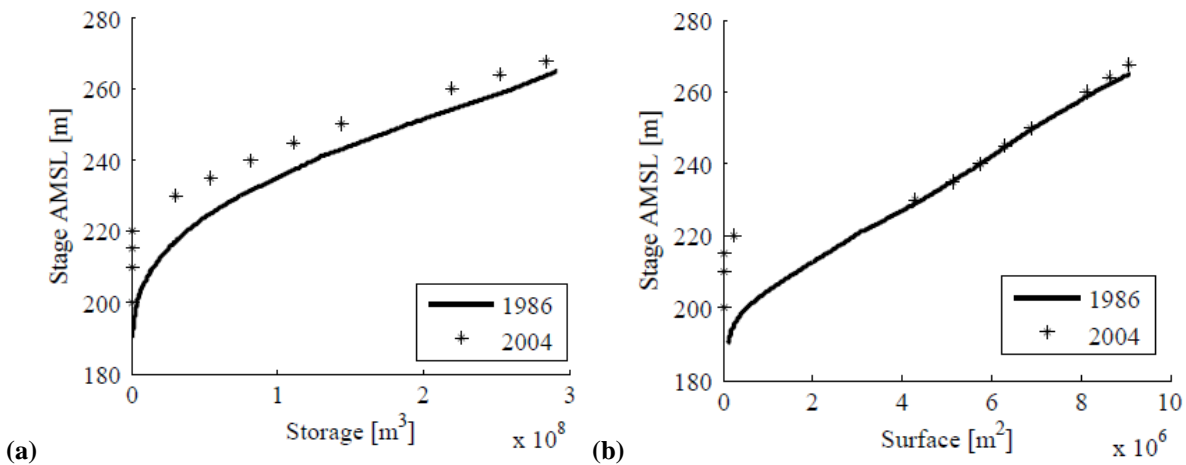


**Figure 2: Stage-storage (a) and stage-surface (b) relationships for the reservoir in 1986 and 2004.**



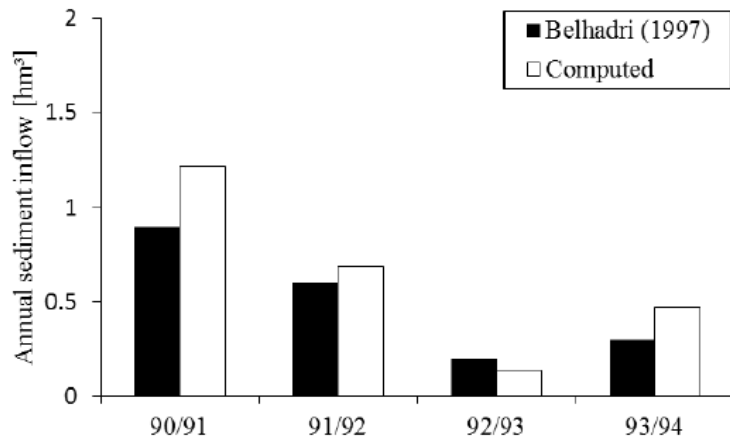


**Figure 3: Comparison between computed annual sediment inflow and values estimated by Belhadri (1997).**

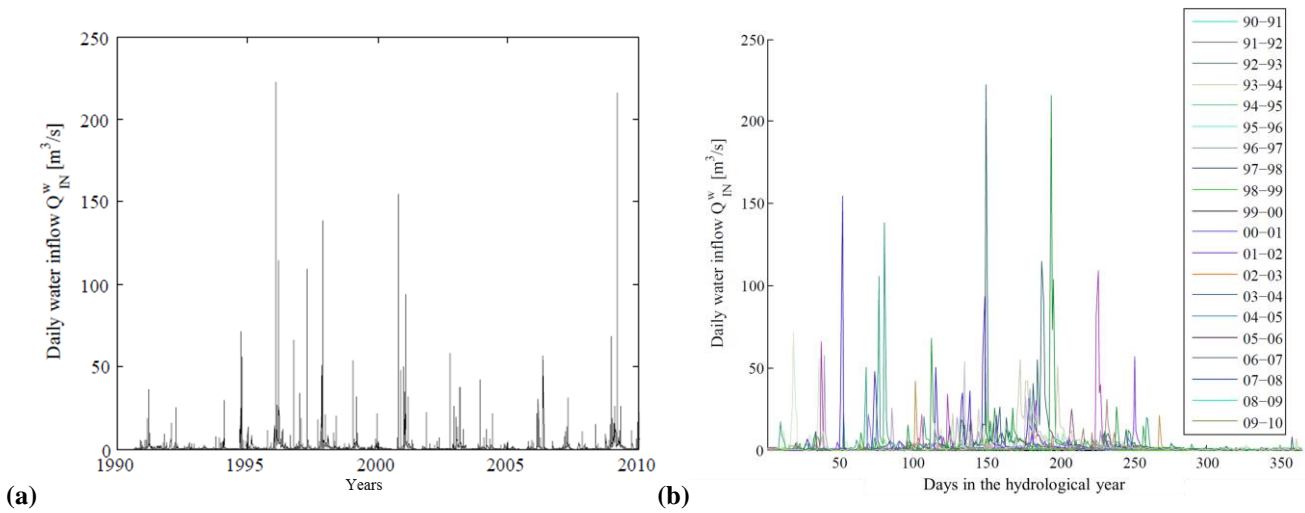


**Figure 4: Computed daily water inflow during the reference period 1990-2010, displayed for the whole period (a) and per hydrological year (b).**

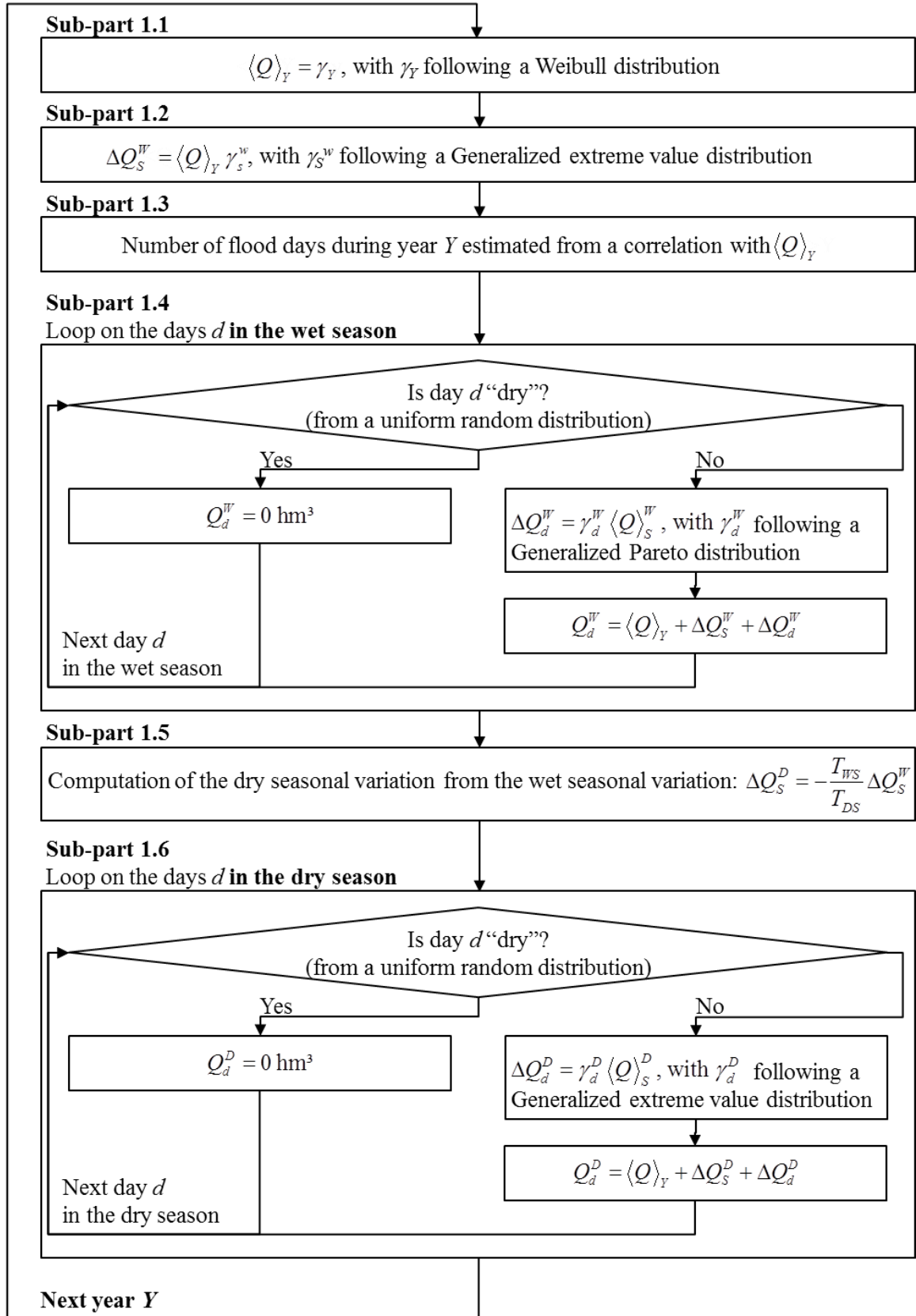
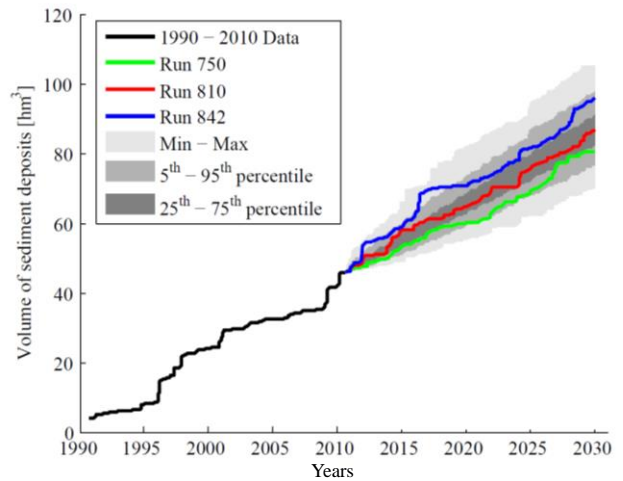
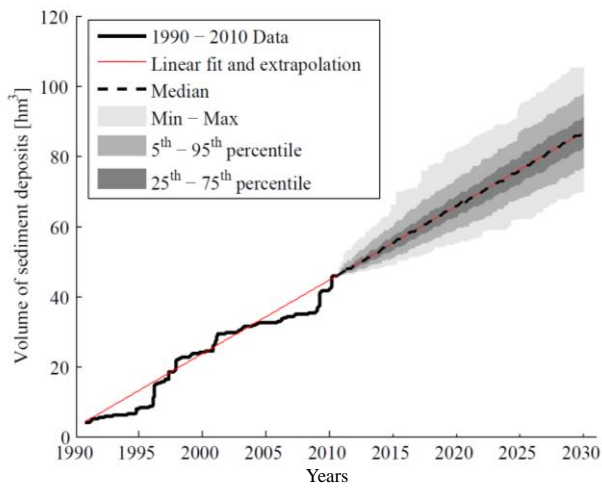


Figure 5: Flow chart describing part 1 of the estimation of future inflows.



(a)

(b)

**Figure 6: Time evolution of the volume of sediment deposits.**

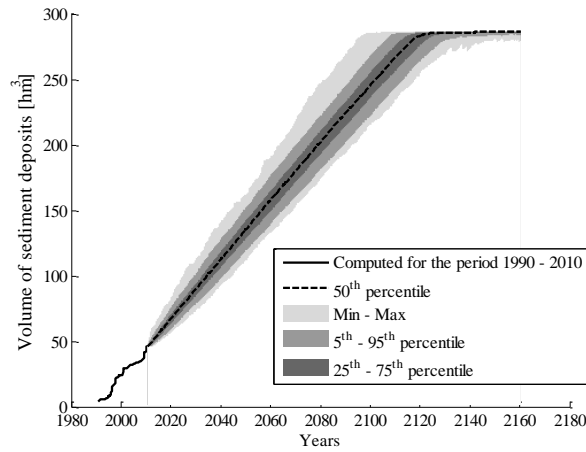
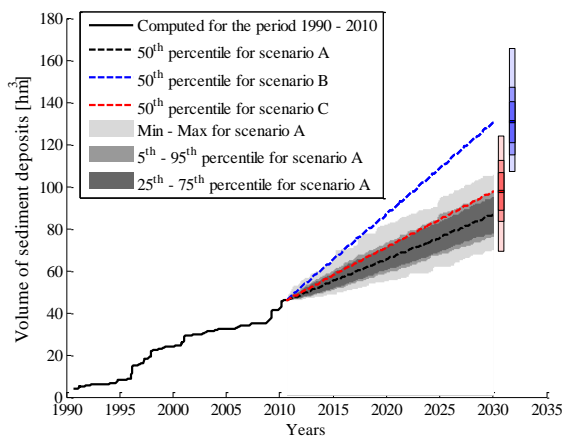
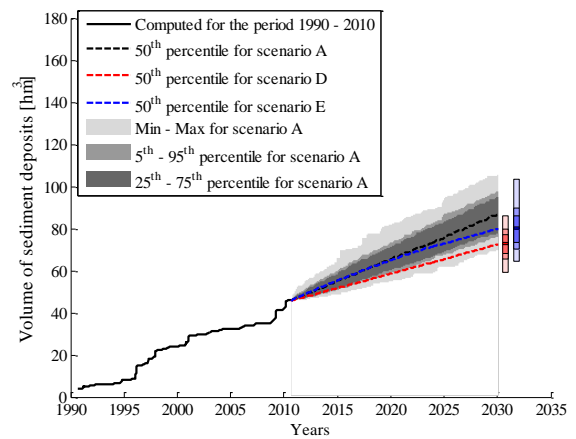


**Figure 7: Long term time evolution of the volume of sediment deposits.**



(a)



(b)

**Figure 8: Time evolution of the volume of sediment deposits for different climate scenarios (a) and different scenarios of erosion control measures in the watershed (b).**